AGU PUBLICATIONS

JGR

Journal of Geophysical Research: Atmospheres

RESEARCH ARTICLE
10.1002/2014JD022301

Key Points:
- Emissions of mineral aerosols and sulfur dioxide are intensive over China
- Sulfate enhanced by aqueous and catalyzed oxidation, heterogeneous uptakes
- Full treatments of mineral aerosol effects on sulfate production are important

Supporting Information:
- Readme
- Tables S1–S6 and Figures S1–S3

Correspondence to:
Y. Song and T. Zhu,
songyu@pku.edu.cn;
tzhu@pku.edu.cn

Citation:
Huang, X., Y. Song, C. Zhao, M. Li, T. Zhu, Q. Zhang, and X. Zhang (2014), Pathways of sulfate enhancement by natural and anthropogenic mineral aerosols in China, *J. Geophys. Res. Atmos.*, *119*, 14,165–14,179, doi:10.1002/2014JD022301.

Received 12 JUL 2014
Accepted 30 NOV 2014
Accepted article online 3 DEC 2014
Published online 20 DEC 2014

Pathways of sulfate enhancement by natural and anthropogenic mineral aerosols in China

Xin Huang[1,2], Yu Song[1], Chun Zhao[3], Mengmeng Li[1], Tong Zhu[1], Qiang Zhang[4], and Xiaoye Zhang[5]

[1]State Key Joint Laboratory of Environmental Simulation and Pollution Control, Department of Environmental Science, Peking University, Beijing, China, [2]Institute for Climate and Global Change Research & School of Atmospheric Sciences, Nanjing University, Nanjing, China, [3]Atmospheric Science and Global Change Division, Pacific Northwest National Laboratory, Richland, Washington, USA, [4]Ministry of Education Key Laboratory for Earth System Modeling, Center for Earth System Science, Institute for Global Change Studies, Tsinghua University, Beijing, China, [5]Key Laboratory for Atmospheric Chemistry, Chinese Academy of Meteorological Sciences, CMA, Beijing, China

Abstract China, the world's largest consumer of coal, emits approximately 30 million tons of sulfur dioxide (SO_2) per year. SO_2 is subsequently oxidized to sulfate in the atmosphere. However, large gaps exist between model-predicted and measured sulfate levels in China. Long-term field observations and numerical simulations were integrated to investigate the effect of mineral aerosols on sulfate formation. We found that mineral aerosols contributed a nationwide average of approximately 22% to sulfate production in 2006. The increased sulfate concentration was approximately 2 $\mu g\,m^{-3}$ in the entire China. In East China and the Sichuan Basin, the increments reached 6.3 $\mu g\,m^{-3}$ and 7.3 $\mu g\,m^{-3}$, respectively. Mineral aerosols led to faster SO_2 oxidation through three pathways. First, more SO_2 was dissolved as cloud water alkalinity increased due to water-soluble mineral cations. Sulfate production was then enhanced through the aqueous-phase oxidation of S(IV) (dissolved sulfur in oxidation state +4). The contribution to the national sulfate production was 5%. Second, sulfate was enhanced through S(IV) catalyzed oxidation by transition metals. The contribution to the annual sulfate production was 8%, with 19% during the winter that decreased to 2% during the summer. Third, SO_2 reacts on the surface of mineral aerosols to produce sulfate. The contribution to the national average sulfate concentration was 9% with 16% during the winter and a negligible effect during the summer. The inclusion of mineral aerosols does resolve model discrepancies with sulfate observations in China, especially during the winter. These three pathways, which are not fully considered in most current chemistry-climate models, will significantly impact assessments regarding the effects of aerosol on climate change in China.

1. Introduction

Sulfate is one of the most effective radiative-cooling aerosols in the atmosphere. It scatters sunlight. Some of the sunlight is lost in space, reducing solar irradiance at the top of the atmosphere. Additionally, sulfate can act as cloud condensation nuclei and modify clouds' microphysical properties, subsequently influencing the radiation budget [*Charlson et al.*, 1992; *Haywood and Boucher*, 2000; *Karl and Trenberth*, 2003]. This radiative-cooling effect may be sufficient to partially or completely offset the positive forcing from greenhouse gases and black carbon (BC) [*Kiehl and Briegleb*, 1993; *Stocker et al.*, 2013].

China has been experiencing an economic boom in recent decades, with a dramatic increase in the amount of energy consumption. In 2012, China consumed approximately 3.6 billion tons of coal equivalent energy [*National Bureau of Statistics of China*, 2013]. Coal combustion, which constitutes approximately 70% of the primary energy consumption, is and will continue to be the major component of energy supply for the foreseeable future in China [*You and Xu*, 2010]. This large consumption of coal results in a total of approximately 30 million tons of sulfur dioxide (SO_2) emissions annually [*Lu et al.*, 2011; *Zhang et al.*, 2012a], which leads to a tremendous sulfate yield. An extremely heavy sulfate burden of more than 20 $\mu g\,m^{-3}$ is observed in most areas in China. In some places, sulfate burden reaches 40 $\mu g\,m^{-3}$ perennially [*Zhang et al.*, 2012b]. This large amount of sulfate has led to significant surface dimming and impacts the regional climate in China [*Qian and Giorgi*, 1999; *Qian et al.*, 2009].

Sulfate is an atmospheric oxidation product of SO_2 in gas and aqueous phases. In the gas phase, SO_2 is oxidized by the hydroxyl radical (•OH) to produce sulfuric acid (H_2SO_4), which condenses to form sulfate. SO_2 can be dissolved in cloud water and react with dissolved ozone (O_3), hydrogen peroxide (H_2O_2), hydroxyl radical, organic peroxides, and various oxides of nitrogen [*Seinfeld and Pandis*, 2006]. These reactions are often considered in photochemical transport models. However, modeling studies significantly underestimated sulfate concentrations by factors of 2 or more in East Asia [*Jiang et al*., 2013; *Park et al*., 2014; *Pozzer et al*., 2012]. Although the underestimation of SO_2 and primary sulfate could explain the discrepancy between measured and modeled sulfate levels, *Zhang et al*. [2009] estimated that the uncertainty was only ±12% for China's SO_2 emissions in 2006. The systematic tendency of the model to underestimate sulfate could probably be attributed to the absence of a nonphotochemical pathway to convert SO_2 to sulfate.

Observational studies have proposed potential enhancements of sulfate production due to mineral aerosols. Long-term measurements and intensive campaigns indicated a high consistency between sulfate and calcium or iron in Asia, particularly during winter [*Arimoto et al*., 2004; *Li et al*., 2013; *Wang et al*., 2012]. In situ aircraft studies over the coast of the Japan Sea revealed that the concentration of sulfate tended to increase whenever soluble calcium (Ca^{2+}) was detected [*Mori et al*., 1999]. Massive productions of sulfate during volcanic eruptions was related to alkaline cloud water neutralized by calcium-rich mineral dust, especially when the overall atmospheric oxidizing capacity was low [*Bao et al*., 2010]. Higher alkalinity in cloud water could benefit SO_2 dissolution, and more S(IV) (dissolved sulfur in oxidation state +4) in aqueous phases is oxidized to sulfate by O_3 and H_2O_2. Nitrogen dioxide (NO_2) could also be a significant oxidant under high ammonia (NH_3) and NO_2 concentrations [*Pandis and Seinfeld*, 1989; *Seinfeld and Pandis*, 2006]. Moreover, atmospheric mineral ions, such as iron (Fe) and manganese (Mn), cause rapid catalyzed oxidation on dissolved S(IV), particularly when both elements are present. For typical atmospheric concentrations of iron and manganese, the synergistic effect raises the catalyzed oxidation rate of sulfur in clouds several times over the rate of iron separately [*Brandt and van Eldik*, 1995; *Martin and Good*, 1991; *Martin et al*., 1991]. Evidence for the catalyzed oxidation also exists from laboratory studies, field measurements, and numerical modeling [*Alexander et al*., 2009; *Harris et al*., 2013; *Martin et al*., 1991]. Numerous studies performed bulk and single-particle analyses to provide direct proof for SO_2 oxidation and sulfate formation on mineral aerosols [*Bates et al*., 2004; *Bauer and Koch*, 2005; *Goodman et al*., 2001; *Hwang and Ro*, 2006; *Li et al*., 2006; *Matsuki et al*., 2005; *Sullivan et al*., 2007; *Usher et al*., 2003; *Zhang and Iwasaka*, 1999; *Zhang et al*., 2006]. Additionally, field studies have shown that mineral dust particles are often coated with sulfate [*Levin et al*., 1996; *Li et al*., 2011; *Song et al*., 2005]. Some numerical models have treated the SO_2 heterogeneous reactions and found that it is important to produce sulfate [*Dentener et al*., 1996; *Fairlie et al*., 2010; *Liao et al*., 2003; *Manktelow et al*., 2010].

Mineral aerosol loadings are extremely high in China, resulting from both natural sources (e.g., windblown dust from soil) and anthropogenic causes (e.g., coal fly ash, cement production, construction activities). Northern China has many deserts, Gobi deserts, and arid loess lands and thus is one of the world's largest mineral dust sources [*Zhang et al*., 1997]. The annual mean dust emission (less than 10 μm in aerodynamic diameter) was estimated to be 8.4 Tg in northern China [*Xuan and Sokolik*, 2002]. Extensive coal combustion, industrial processes, and construction activities also emit a large quantity of alkaline materials that have similar chemical components as soil dust in China [*Dai et al*., 2010]. Annual primary anthropogenic PM_{10} (particles in the ambient air, with 10 μm or less in aerodynamic diameter) emissions reached 18.8 Tg in 2005, the majority of which was composed of minerals [*Lei et al*., 2011]. Mineral aerosols may enhance sulfate production in China through aqueous oxidation by increasing dissolved S(IV) in cloud water due to alkaline mineral materials, oxidized both by O_3, NO_2, and H_2O_2 and by transition metal catalysis, and through heterogeneous reactions. However, these three pathways are not fully considered in most atmospheric chemical transport models (Table S1 in the supporting information).

We integrated field measurements and numerical simulations to investigate the relative importance of mineral aerosols on sulfate production. First, we measured sulfate and mineral aerosols at 14 sites across China in 2006. Additionally, we used the Weather Research and Forecasting model coupled with Chemistry (WRF-Chem) to get a better idea of the contributions of mineral aerosols in sulfate formation. Three SO_2 oxidation pathways related to mineral aerosols were investigated: (1) aqueous-phase oxidation of S(IV) by O_3, H_2O_2, and NO_2 with more dissolved SO_2 in cloud water caused by water-soluble mineral cations,

Table 1. WRF-Chem Configuration Options and Settings

	Values/Details
Domain setting	
Horizontal grid	95 × 110
Grid spacing	50 km × 50 km
Vertical layers	15 eta levels
Map projection	Lambert conformal conic
Configuration options	
Longwave radiation	RRTMG (rapid radiative transfer model)
Shortwave radiation	RRTMG
Cumulus parameterization	Grell-Deveny
Land surface	Noah
Boundary layer	YSU
Microphysics	Lin et al.
Photolysis	Fast-J
Gas chemistry	CBMZ
Aerosol chemistry	MOSAIC

(2) S(IV)-catalyzed oxidation in aqueous phases by transition metals rich in combustion mineral aerosols, and (3) SO_2 heterogeneous reactions on the surface of mineral aerosols.

2. Model Description

2.1. WRF-Chem Model

WRF-Chem version 3.4.1 was used to investigate the enhancement role of mineral aerosols in sulfate formation. The simulations were performed on a domain at 50 km horizontal resolution covering China and its surrounding areas with 95 × 110 grid cells. Fifteen vertical layers for all of the grid meshes were used from the ground level to the top pressure of 50 hPa. The initial meteorological fields and boundary conditions were from the 6 h NCEP (National Centers for Environmental Prediction) global final analysis with a 1° × 1° spatial resolution. The simulation was conducted for all of 2006, and each run covered 36 h with a 12 h spin-up time. The CBMZ (Carbon Bond Mechanism) photochemical mechanism and MOSAIC (Model for Simulating Aerosol Interactions and Chemistry) aerosol model are used in this study [*Fast et al*., 2006]. More domain settings and configuration options are in Table 1. In this simulation, some surface parameters in WRF were updated because the default data sets were outdated because of the rapid land use change in China (urbanization, desertification, afforestation, and deforestation). Consequently, we used the MODIS (Moderate-resolution Imaging Spectroradiometer) land use data (MCD12Q1), water mask data (MOD44W), and the Normalized Difference Vegetation Index data (MOD13A2) to deduce the land use types and green vegetation fraction. These updated surface parameters could improve the meteorological simulation, as discussed in *Li et al*. [2014].

The DUSTRAN dust emission module embedded in WRF-Chem included the soil type, soil moisture, and vegetation cover in vertical dust flux calculation [*Shaw et al*., 2008; *Zhao et al*., 2010]. In our simulation, the dust source regions were pinpointed and delineated by four different soil types based on the Harmonized World Soil Database and the Chinese desert maps (Figure S1). Dust was more prone to be emitted on sand and Gobi land, followed by loess, and mixed soil. The dust emission scheme was evaluated by comparing simulation results and the PM_{10} concentration measured at Duolun and Yulin in April 2006, which are located in Inner Mongolia and Shaanxi province, respectively (Figure S2). The comparisons showed that the DUSTRAN dust emission module could reproduce the dust events well.

2.2. Emission Inventory

Typical anthropogenic emissions, including power plant, industrial, residential, and vehicle emissions, were from the MEIC (Multi-resolution Emission Inventory for China; see www.meicmodel.org) database (for China) and Intercontinental Chemical Transport Experiment-Phase B (INTEX-B) Asia emission inventory data set (for surrounding countries) [*Zhang et al*., 2009]. Both the ammonia emissions and biomass burning emissions were updated in China using a bottom-up method [*Huang et al*., 2012a, 2012b; *Song et al*., 2010]. Recent studies showed that the ammonia emissions inventory in *Huang et al*. [2012a] had a similar spatial pattern with the measurements from an Infrared Atmospheric Sounding Interferometer [*Van Damme et al*., 2014] and were close to those derived using an inversion of ammonium wet deposition data [*Paulot et al*., 2014].

2.3. Simulation Experiment

Four parallel experiments were performed. In Experiment I, photochemical oxidation of SO_2 by radicals and aqueous oxidation of S(IV) by dissolved O_3, H_2O_2, and NO_2 were taken into consideration. Soluble mineral cations and transition metals were excluded. In Experiment II, the mineral cations were included based on Experiment I to look into the sulfate production enhanced by aqueous oxidation. Similar to Experiment I, catalyzed oxidation by transition metals in aqueous phases was not included. Mineral aerosols contain

soluble materials (slightly soluble calcium salts, such as $CaCO_3$). Additionally, heterogeneous reactions between acid gases and minerals lead to significant increases in water-soluble calcium, magnesium, and aluminum [*Cao et al*., 2013; *Duvall et al*., 2008; *Hsu et al*., 2014]. The inclusion of water-soluble minerals could increase the cloud water alkalinity, affecting SO_2 dissolution and the rate of aqueous-phase oxidation of S(IV), especially for O_3 and NO_2 [*Seinfeld and Pandis*, 2006]. We used the average value from our in situ measurements across China (Table S2) as the soluble mineral aerosols in the model.

In Experiment III, the S(IV) aqueous oxidation by O_2 catalyzed by Fe(III) and Mn(II) was included based on Experiment II to study the sulfate enhancement from transition metals rich in coal fly ashes [*Chen et al*., 2012]. *Sullivan et al*. [2007], using an online single-particle mass spectrometer, found that sulfate was enriched when internally mixed with Fe/Al-rich mineral dust particles. They suggested that transition metal catalysis of S(IV) to S(VI) could be an important pathway for sulfate production on mineral dust. *Harris et al*. [2012, 2013] also found similar results using isotopic analysis. According to the existing observations in Beijing, Shanghai, Chongqing, Jinan, and Guangzhou, particulate Fe and Mn contributed 2–10% and 0.2–0.6%, respectively, to the total mineral aerosol mass [*Chen et al*., 2006; *Yang et al*., 2012; *Yao et al*., 2002; *Ye et al*., 2003], as listed in Table S3. The dissolved Fe(III) and Mn(II) were calculated using equations (1) and (2).

$$[\mathrm{Fe(III)}] = C \times Q_{\mathrm{Fe}} \times S_{\mathrm{Fe}} \times F \tag{1}$$

$$[\mathrm{Mn(III)}] = C \times Q_{\mathrm{Mn}} \times S_{\mathrm{Mn}} \tag{2}$$

where C is the mass load of the mineral aerosol and Q_{Fe} and Q_{Mn} are the mass fractions of Fe and Mn in mineral aerosols based on field measurements, which are 5.0% and 0.3%, respectively. S_{Fe} and S_{Mn} are the solubility of ambient Fe and Mn and are 10% and 50%, respectively. The iron solubility in soil dust was found to be low, although the solubility was substantially higher in coal fly ash [*Chen et al*., 2012; *Jickells et al*., 2005]. Manganese was typically more soluble than iron and existed mainly as Mn(II) in cloud/fog water. The value used in this estimation was derived from an extensive compilation of aerosol Fe and Mn solubility estimates for samples collected around the globe (Table S4). All of the dissolved Mn was assumed to be Mn(II). Soluble Fe(II) and Fe(III) were found in cloud water [*Siefert et al*., 1998]. In the daytime, Fe(II) was the predominant form of soluble Fe because Fe(III) is reduced to Fe(II) by reacting with superoxide ($O_2{\cdot}^-$). $Fe(OH)_2{}^+$ could be the predominant form of soluble Fe at night, which is when Fe(II) is oxidized by H_2O_2 and hydroxyl radicals. Fe(III) was assumed to be 90% (F in equation (1)) of the dissolved Fe at night and 10% during the day because iron cycles diurnally and exists primarily as Fe(II) during the day and Fe(III) at night [*Siefert et al*., 1998].

In Experiment IV, heterogeneous reactions between SO_2 and mineral aerosols were included based on Experiment III. Soil-derived dust and coal fly ash in China were found to be aluminum-rich and calcium-rich, mainly as Al_2O_3, CaO, and $CaMg(CO_3)_2$ [*Dai et al*., 2010; *Winchester et al*., 1981], which are the most reactive alkaline mineral species for SO_2 partitioning [*Goodman et al*., 2001; *Li et al*., 2006; *Zhang et al*., 2006]. Such heterogeneous reactions may be more significant in China than in other regions. A first-order SO_2 uptake parameterization on surface of mineral aerosols [*Ullerstam et al*., 2003; *Usher et al*., 2003] was assumed and is denoted in equation (3).

$$k_i = \int_{r1}^{r2} 4\pi r^2 \Big/ \left(\frac{r}{Dg} + \frac{4}{v\gamma}\right) \frac{dN}{dr} dr \tag{3}$$

where k_i is the apparent rate constant for size bin i, dN/dr denotes the concentration of mineral dust in size i (radius range from r_1 to r_2), Dg is the diffusivity (0.15 $cm^2 s^{-1}$), and v is the mean molecular speed (3.0×10^4 cm s^{-1}). We chose the uptake coefficients (γ) to be 1×10^{-4} under general conditions and 5×10^{-4} for high humidity (RH > 80%) according to previous studies on the interaction between SO_2 and the minerals (listed in Table S5).

2.4. PM_{10} Chemical Measurements

The simulated mineral cation and sulfate concentrations would be evaluated with the ambient PM_{10} measurements. Twenty-four-hour ambient PM_{10} filter samples were collected every 3 days at 14 urban and rural stations across China in 2006 (Figure S3). Samples were collected with a MiniVol air sampler (Airmetrics, Oregon, USA), operating at an ambient air flow rate of 5 l min^{-1} for 24 h from 09:00 A.M. to 09:00 A.M. (Beijing time) the following day. Mineral aerosols were analyzed using X-ray fluorescence (XRF) with an X-Lab 2000

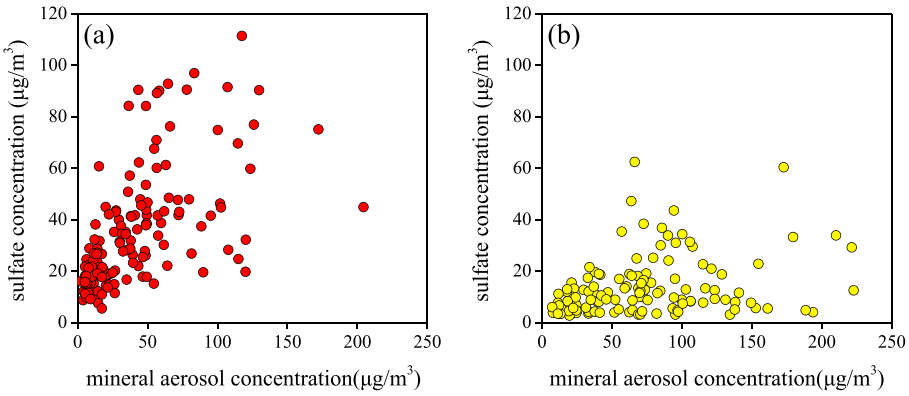

Figure 1. Correlation between sulfate and mineral aerosol concentrations under (a) humid conditions (relative humidity greater than 70%) during the winter of 2006 and (b) dry conditions (relative humidity less than 40%) during whole year.

(SPECTRO,Germany) instrument. After the XRF analysis, a portion of the filter samples were allocated to determine the sulfate concentration using ion chromatography (Dionex 600 series). The details of method and data are documented in *Zhang et al.* [2012b].

3. Results

3.1. Mineral Aerosol and Sulfate Observations

Measured mass concentrations of mineral aerosols in PM_{10} were high and showed a distinct seasonal variation at 14 monitoring stations. Northern China suffered from grievous pollution, especially during the spring and winter. The mineral aerosol concentrations only exceeded 85 $\mu g\, m^{-3}$ during the winter and were greater than 110 $\mu g\, m^{-3}$ during spring in Gucheng, Xian, and Gaolanshan. Mineral aerosol levels in southern China, such as in Taiyangshan, Panyu, and Nanning, were generally lower than 40 $\mu g\, m^{-3}$ throughout the year. The spatial variations were caused by different meteorological conditions and varied anthropogenic and natural emission intensity. Dust regions are predominately concentrated in northern China, specifically, Inner Mongolia, Xinjiang, and the Gansu Province. Additionally, anthropogenic sources, such as industrial manufacturers and power plants, were relatively denser in the Hebei, Shandong, and Henan Provinces [*Zhang et al*., 2009]. Seasonal patterns of mineral aerosol concentrations were substantially different between northern and southern China. Mineral aerosols peaked during winter and spring in northern China but experienced less fluctuation in southern regions. The disparity was mainly caused by meteorology-dependent dust emissions and different heating demands. Spring is the worst dust-emitting season with half of the annual emission amounts [*Xuan and Sokolik*, 2002]. Mineral aerosols reached their maximum in northern China where the impact of dust emissions is remarkable. In winter, massive emissions and large amounts of fossil fuel consumption for heating resulted in high concentrations of mineral aerosols in northern China [*Zhao et al*., 2006]. These two factors were much less significant in southern China.

Large amounts of sulfates were found in Gucheng, Zhengzhou, Xian, and Chengdu, where the annual averaged mass concentrations exceeded 40 $\mu g\, m^{-3}$. The corresponding concentrations were approximately 20 $\mu g\, m^{-3}$ at southern stations, such as Panyu, Nanning, and Linan, and decreased to less than 10 $\mu g\, m^{-3}$ in remote regions (Lasha, Gaolanshan, and Dunhuang). Seasonally, sulfate levels at the northern stations rose rapidly during the winter. The large increase during winter was not obvious at the southern stations. As a secondary component, sulfate production is commonly determined by SO_2 levels and its subsequent transformation. The former is primarily due to anthropogenic activities, such as fossil fuel combustion, while the latter is highly dependent on meteorology and ambient substances involved in SO_2 oxidation. Sulfates exhibited a strong positive relationship with mineral aerosols under humid conditions (Figure 1a) and a weak relationship under dry conditions (Figure 1b). SO_2 can be effectively oxidized to sulfate by aqueous and heterogeneous reactions, which are more active when the humidity is high [*Seinfeld and Pandis*, 2006]. The mineral aerosol's enhancement effect in sulfate production may be more important during the winter and summer when the relative humidity is often high in China.

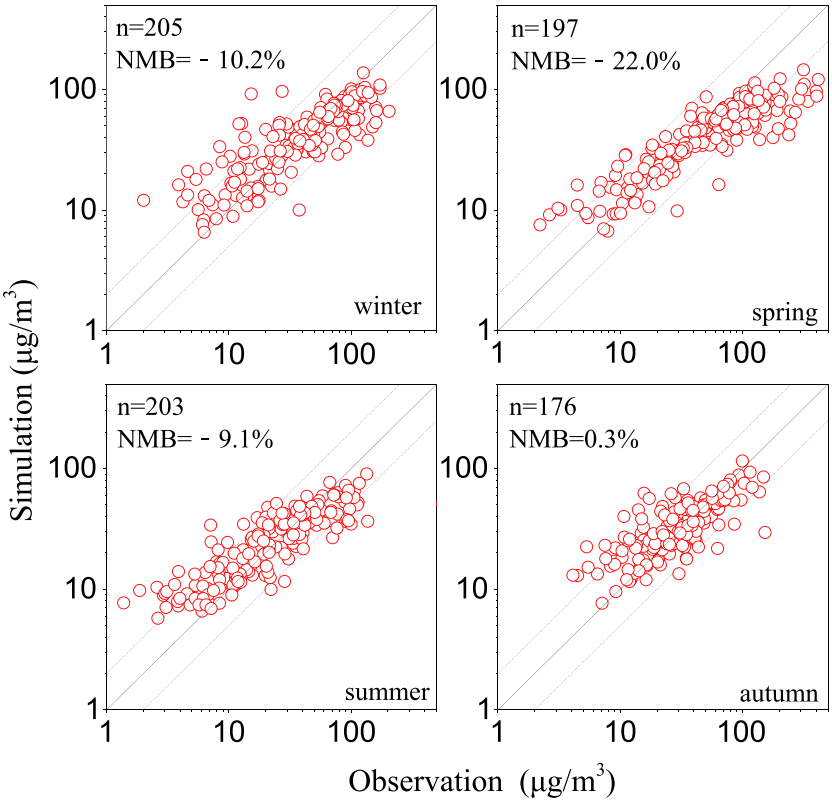

Figure 2. Scatterplots of the daily averages of the simulated and the observed mass concentrations of mineral aerosols. Letter n represents the number of samples; NMB represents the normalized mean bias.

3.2. Model Evaluation

Meteorology plays an important role in aerosol transport, diffusion, and chemical reactions in the atmosphere. Simulated meteorological fields were evaluated using available daily temperature and relative humidity observations at 2 m (T2 and RH2) at 839 stations in 2006 from the China Meteorological Data (website: cdc.cma.gov.cn). Simulated results were compared with observations in terms of performance statistics (Table S6). Generally, the model reproduced temporal variations and spatial distributions of T2 and RH2. The temperature was underpredicted (0.7°C) during the winter, but the biases were smaller during the other three seasons (−0.5°C ~ −0.6°C). The mean biases of simulated RH2 were less than ±4% during the four seasons.

Simulated mineral aerosol concentrations were compared with our measurements in Figure 2, which were consistent in both magnitude and seasonal patterns with higher concentrations during the winter and spring. Figure 3 shows a comparison of measured and simulated annual mean mineral cation concentrations. The mineral cation concentrations were reproduced during this simulation. The model and the measurements showed heavier mineral cation loadings at northern stations, such as Gucheng and Zhengzhou. Simulated mineral cation concentrations in cloud water were compared with observations from four aircraft measurements (Table 2). High mineral cation concentrations (exceeding 30 μmol L^{-1}) were observed in cloud water at both the Changchun and Chongqing sites. The cation concentrations were underpredicted at the two sites, which is likely because the emissions from construction activities were not included in our simulations. The modeled pH values of cloud water showed an increase of approximately 0.7 after including the mineral cations. The simulated atmospheric iron concentrations, which were at the maximum during winter and spring and decreased rapidly in the summer, agreed with the measurements in terms of spatial distribution and seasonal variation (Table 3).

Based on well-characterized meteorological conditions and mineral aerosol concentrations, we aimed to quantify the enhancement of mineral aerosols on sulfate production. Figure 4 shows a remarkable increase in

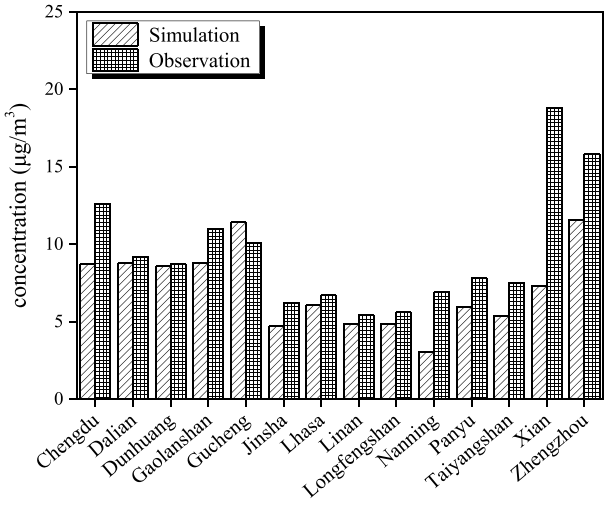

Figure 3. Comparison of the simulated and the observed mineral cation concentrations.

simulated sulfate concentrations because of the involvement of mineral aerosols. The model's sulfate estimations were much better in Experiment IV compared to those in Experiment I and previous simulations [*Park et al.*, 2014; *Wang et al.*, 2012]. Experiment I significantly underestimated the sulfate concentrations during the winter, with a NMB (normalized mean bias) of −60.6%. Including the mineral aerosol's effect in Experiment IV reduced the corresponding NMB to −36.0%. For spring and autumn, the modeled sulfate concentrations also showed fewer gaps with corresponding observations in Experiment IV. The simulation results showed that winter is when mineral aerosols exerted a more obvious impact on sulfate production.

3.3. Pathways of Sulfate Enhancement due to Mineral Aerosol

Figure 5 shows a comparison of a time series of the simulated daily averaged sulfate concentrations and the corresponding observations at three typical sites (locations are labeled in Figure S1): Gucheng (39°8′N, 115°48′E, located in the North China Plain), Linan (30°18′N, 119°44′E, located in the Yangtze Delta Plain), and Nanning (22°49′N, 108°21′E, located in southern China).

At Gucheng, where a dense rural population exists and numerous industrial plants are located, the annual mean sulfate concentration was 36 $\mu g\,m^{-3}$ and rose to approximately 45 $\mu g\,m^{-3}$ during the winter; Experiment I substantially underestimated the observed sulfate concentrations when the effect of mineral aerosols was excluded. Experiment IV, which included this effect, reduced this bias. The modeled annual mean mineral aerosol and SO_2 concentrations were 83 $\mu g\,m^{-3}$ and 14 ppb, respectively. The simulation results showed that the presence of concentrated mineral aerosols was important for SO_2 transformation, raising the annual and average winter sulfate concentrations by 6.7 and 9.5 $\mu g\,m^{-3}$, respectively. The enhanced aqueous oxidation and heterogeneous reactions contributed equally to the sulfate production. Compared to Gucheng, the gap between Experiment I and the observations was less notable at Linan. Linan is close to the East China Sea and had a high annual average relative humidity of over 70%. Although it was less polluted with mineral aerosol and SO_2 concentrations of 32 $\mu g\,m^{-3}$ and 7 ppb, respectively, the humid conditions made mineral aerosols important to the aqueous oxidation of S(IV). Mineral aerosols zincreased the annual mean sulfate concentration by 5.6 $\mu g\,m^{-3}$ through aqueous oxidation by increase in alkalinity of cloud water, transition metal-catalyzed oxidation, and heterogeneous uptake. Experiments I and IV had a small disparity at Nanning, and both of them agreed with our measurements. Nanning, in southern China, was less affected by both anthropogenic activities and natural dust emissions. The city has one of the best air quality ratings in China. The interaction between mineral aerosols and sulfate formation became much less notable because of the low mineral aerosol and SO_2 concentrations

Table 2. Comparison of the Modeled and Observed pH Values of Cloud Water and Ca^{2+} Concentrations in Cloud Water

	Mineral Cation Concentrations in Cloud Water ($\mu mol\,l^{-1}$)		Ph Value Of Cloud Water		
Locations	Observation[a]	Simulation	Observation[a]	Experiment I	Experiment II
Shanghai	2.1	7.2	4.8-5.8	3.6	4.1
Changchun	36.0	25.0	4.9	3.5	4.2
Chongqing	49.0	17.8	4.6	3.1	3.8
Guiyang	16.0	10.2	4.7	3.6	3.9

[a]Observations are derived from *Shen et al.* [1993], *Xue et al.* [2010], and *Zhang et al.* [1991].

Table 3. Comparison of the Simulated and the Observed Atmospheric Iron Concentrations ($\mu g\ m^{-3}$)

Locations (Season)	Simulations	Observations[a]
Minqing (spring)	3.4	3.6
Minqing (summer)	2.0	2.9
Qingdao (spring)	2.2	2.8
Qingdao (summer)	0.5	1.5
Qingdao (autumn)	1.1	3.0
Qingdao (winter)	1.6	3.8
Beijing (spring)	2.2	1.6
Beijing (summer)	1.2	0.7
Beijing (autumn)	2.0	2.0
Beijing (winter)	2.0	1.6
Shanghai (spring)	1.5	1.0
Shanghai (summer)	0.9	0.7
Shanghai (autumn)	1.0	0.9
Shanghai (winter)	1.4	1.0

[a]Observations are derived from *Hao et al.* [2007], *Liu et al.* [2002], *Ye et al.* [2003], and *P. S. Zhao et al.* [2013].

($24\ \mu g\ m^{-3}$ and 3 ppb, respectively). The annual mean sulfate concentration was $15\ \mu g\ m^{-3}$, of which sulfate production enhanced by mineral aerosols contributed less than 20%.

Figure 6 demonstrates the relative contributions of these three sulfate enhancement pathways related to mineral aerosols in China during different seasons. Without considering the effects of mineral aerosols, the sulfate production pathways include SO_2 oxidation by the hydroxyl radical in the gas phase and S(IV) oxidation by O_3, H_2O_2, and NO_2 in the aqueous phase. These pathways accounted for 78% of the total sulfate throughout the year. Considering the effects of mineral aerosols, the enhanced sulfate production contributed approximately 22% of the total sulfate production in China. The contribution was 40% during the winter and 12% during the summer. Therefore, the sulfate enhancement by mineral aerosols cannot be neglected.

The difference between Experiments I and II was the sulfate contribution from Pathway I, that is, an enhanced aqueous-phase oxidation of S(IV) by O_3, H_2O_2, and NO_2 while considering water-soluble mineral cations. The soluble alkaline mineral substances could elevate the pH value in cloud water, which leads to more dissolved SO_2. More sulfates are produced from aqueous-phase oxidation by O_3, H_2O_2, and NO_2. Additionally, higher pH values can increase the rate of aqueous-phase oxidation of S(IV) by O_3, H_2O_2, and NO_2 [*Seinfeld and Pandis*, 2006]. The simulation results showed that Pathway I increased the national mean mass concentration of sulfate by approximately $0.5\ \mu g\ m^{-3}$ and accounted for 5% of the total sulfate concentration. The contributions varied spatially and temporally. In East China, such as Hebei, Shanxi, Shandong, and Henan Provinces (Figure 7a), where SO_2 emissions are very high due to numerous power plants and industrial activities [*Zhang et al.*, 2009] and both nitrogen oxide and gaseous ammonia emissions are very high [*Huang et al.*, 2012b; *Zhang et al.*, 2007], sulfate increased through Pathway I, reaching a concentration as high as $1.2\ \mu g\ m^{-3}$. Moreover, SO_2 concentrations were also high in winter because of residential heating and a stable atmospheric boundary layer. This result implies that the mineral aerosol loadings from combustion sources may also be high. In addition, mineral aerosols can also be contributed by windblown dust from bare soil. Mineral aerosols promote higher alkalinity in cloud water. In summer, turbulent mixing should be stronger, resulting in lower SO_2 concentrations at the surface. However, the humidity and the O_3 and H_2O_2 concentrations are high. These conditions promote SO_2 dissolution and S(IV) oxidation in the aqueous phase. Seasonally, Pathway I made larger contributions to the total sulfate production in winter and summer (5.2% and 5.5%, respectively), which is shown in Figure 6.

Pathway II on sulfate enhancement was related to transition metal-catalyzed oxidation of dissolved SO_2, which was derived from the difference between Experiments II and III. Transition metal-catalyzed oxidation of S(IV) in the aqueous phase can process with oxygen (O_2). Atmospheric transition metals were richer during winter because of the increased heating demand and the low planetary boundary layer height. Table 3 shows that winter atmospheric iron concentrations generally exceeded $1.0\ \mu g\ m^{-3}$, which doubled or even tripled those in summer. According to our work, Pathway II contributed approximately 8% of total sulfate in China, which had a distinct seasonality with a winter maximum (19%) and a summer minimum (2%). Pathway II depends strongly on the ambient liquid water content and transition metal and SO_2 concentrations. As shown in Figure 7b, the contributions from Pathway II were high in the Sichuan Basin, Hubei, Hunan, and Anhui Provinces in central China, and Jiangsu and Zhejiang Provinces in East China. The transition metal concentrations are proportional to the mineral aerosol concentrations, which are primarily emitted from coal fly ashes, especially in winter. The sulfate concentration enhancement due to Pathway II in the Sichuan Basin was remarkable, reaching an annual mean concentration of $4.8\ \mu g\ m^{-3}$; the maximum concentration was found to occur in winter ($11.7\ \mu g\ m^{-3}$). The Sichuan Basin is a region that exhibits stagnant air and high relative humidity throughout the year. These meteorological conditions favor sulfate enhancement via Pathway II.

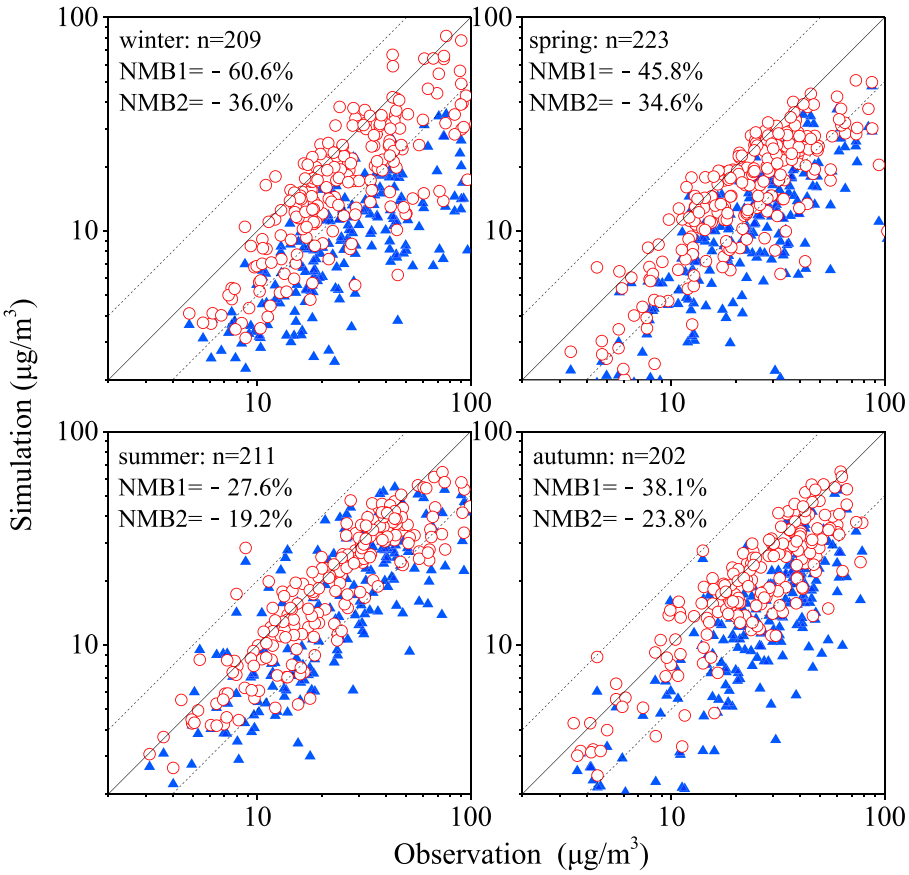

Figure 4. Scatterplots of the daily averages of the simulated and the observed mass concentrations of sulfate. Blue triangles are results of Experiment I, and red circles represent the results of Experiment IV. Letter n is the number of samples; NMB1 and NMB2 are the normalized mean biases for Experiments I and IV, respectively.

The sulfate increase caused by the aforementioned two aqueous-phase oxidation pathways (the sum of Pathways I and II) was high during the winter. Including transition, metal-catalyzed oxidation and mineral cations accounted for 24% of the winter sulfate concentration in China. The inclusion, however, had a negligible effect during the summer when approximately 8% of total sulfate was related to enhanced aqueous oxidation because of mineral aerosols. The contribution from photochemical oxidation of SO_2 was relatively less during the winter because of weaker sunlight. Additionally, high levels of SO_2 and mineral substances during the winter caused by intensive emissions from coal combustion caused by the heating demand, the stable thermal stratification in the boundary layer, and low amounts of precipitation could be other reasons to explain the higher contribution of sulfate from aqueous-phase oxidation.

Pathway III, which was deduced from the gaps between Experiments III and IV, was the SO_2 heterogeneous reactions on the surface of mineral aerosols. The national mean sulfate production increased by 0.8 $\mu g\,m^{-3}$ because of heterogeneous reactions. Pathway III contributed 9% of the annual mean sulfate production. In East China and the Sichuan Basin, which are regions indicative of high SO_2 and mineral aerosol concentrations, Pathway III was responsible for augmented concentrations of 3.0 $\mu g\,m^{-3}$ and 1.9 $\mu g\,m^{-3}$, respectively, or 22% and 14% of the total sulfate concentrations (Figure 7c). Heterogeneous uptake is an effective SO_2 oxidation pathway because both SO_2 and mineral aerosols have high loadings in China. Seasonally, SO_2 heterogeneous reactions on the surface of mineral aerosols were much more important during the winter (16%) and became relatively inactive during the summer (4%). Accumulating SO_2 and minerals during the winter resulted in an increased reaction probability. Additionally, higher relative humidity during the winter intensified the heterogeneous uptake. During summer, however, photochemical oxidation and aqueous oxidation with O_3, H_2O_2, and NO_2 were the dominant pathways of sulfate formation because of

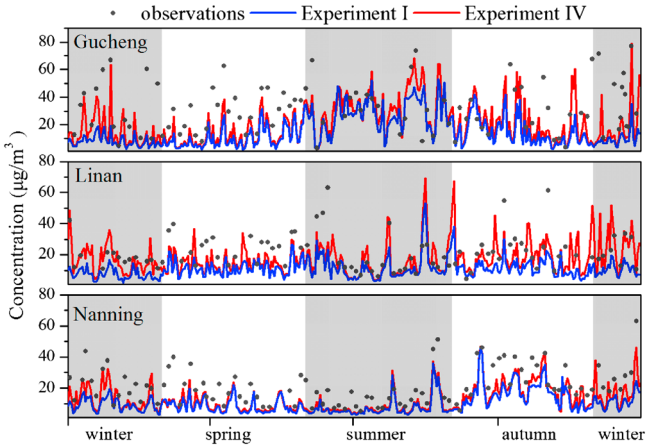

Figure 5. Daily averages of the simulated and the observed mass concentrations of sulfate for 2006 (blue lines: Experiment I; red lines: Experiment IV; black dots: observations).

the soaring atmospheric oxidizing capacity. Fewer emissions and favorable diffusion conditions led to much lower SO_2 and mineral aerosol concentrations. Therefore, the heterogeneous interaction between SO_2 and mineral aerosols was not significant during the summer.

Considering all of the effects from mineral aerosols on sulfate production increased the national mean sulfate concentration by approximately 2 $\mu g\,m^{-3}$. Spatially, the sulfate increase caused by mineral aerosols was much more efficient over East China and the Sichuan Basin with concentrated anthropogenic emissions, where the enhanced sulfate production caused by mineral aerosols was 6.3 $\mu g\,m^{-3}$ and 7.3 $\mu g\,m^{-3}$, respectively (Figure 7d). These two regions are affected by both anthropogenic activities and natural dust emissions. Modeled regional mean mineral aerosol concentrations were as high as 49.5 $\mu g\,m^{-3}$ and 31.3 $\mu g\,m^{-3}$, respectively, in 2006, much denser than other parts of China. East China and the Sichuan Basin have numerous power plants and industrial activities that result in tremendous SO_2 emissions into the atmosphere. In the Sichuan Basin, sulfate production was enhanced by mineral aerosols primarily through Pathway II because aqueous chemistry in cloud water was more active due to the year-round high humidity. However, in northern China, especially in Shandong and Henan Provinces, heterogeneous uptake on mineral aerosol surfaces (Pathway III) may be more important.

Enhanced sulfate production may be linked to the frequent outbreak of winter haze across China; these events typically exhibit sulfate concentrations that are 5 to 15 times higher than normal [*Fu et al.*, 2008; *Sun et al.*, 2006; *X. J. Zhao et al.*, 2013]. Two pronounced haze episodes and one dust storm event were studied to understand the effects of mineral aerosols on sulfate production enhancement. Daily average PM_{10} and sulfate surface concentrations of 339.4 $\mu g\,m^{-3}$ and 46.3 $\mu g\,m^{-3}$, respectively, were observed in Gucheng (located in North China Plain) on 19 January 2006. The visibility in Beijing was only 2.9 km. The corresponding model simulation resulted in a sulfate concentration of 41.1 $\mu g\,m^{-3}$, agreeing with the observation. The stagnant meteorological conditions (wind speed less than 1.0 $m\,s^{-1}$) favored the accumulation of sulfate precursors. The simulated daily average mass concentrations of SO_2 and mineral aerosols were as high as 50.0 ppb and 117.3 $\mu g\,m^{-3}$, respectively. The high humidity (daily average 70%) enhanced aqueous oxidation and the heterogeneous uptake of SO_2 on mineral aerosols. However, without considering the effects of mineral aerosol, the simulated sulfate concentration was merely 17.7 $\mu g\,m^{-3}$ in Gucheng. Pathway I

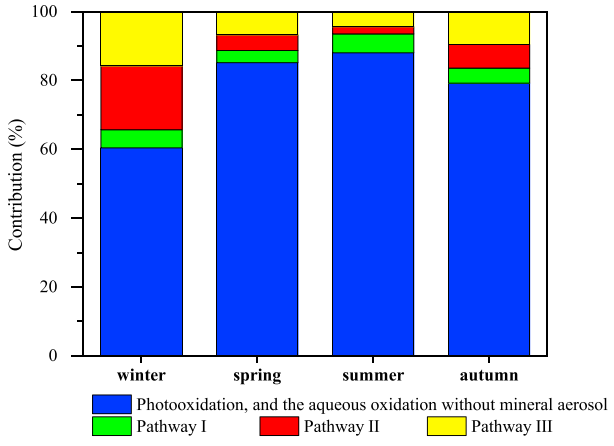

Figure 6. Seasonal contribution of photooxidation and aqueous oxidation without mineral aerosols (blue boxes), enhanced aqueous oxidation by H_2O_2, O_3, NO_2, etc. caused by increasing alkalinity in cloud water by mineral cations (Pathway I, green boxes), transition metal-catalyzed oxidation (Pathway II, red boxes), and heterogeneous reactions on mineral surfaces (Pathway III, yellow boxes) to sulfate production in China.

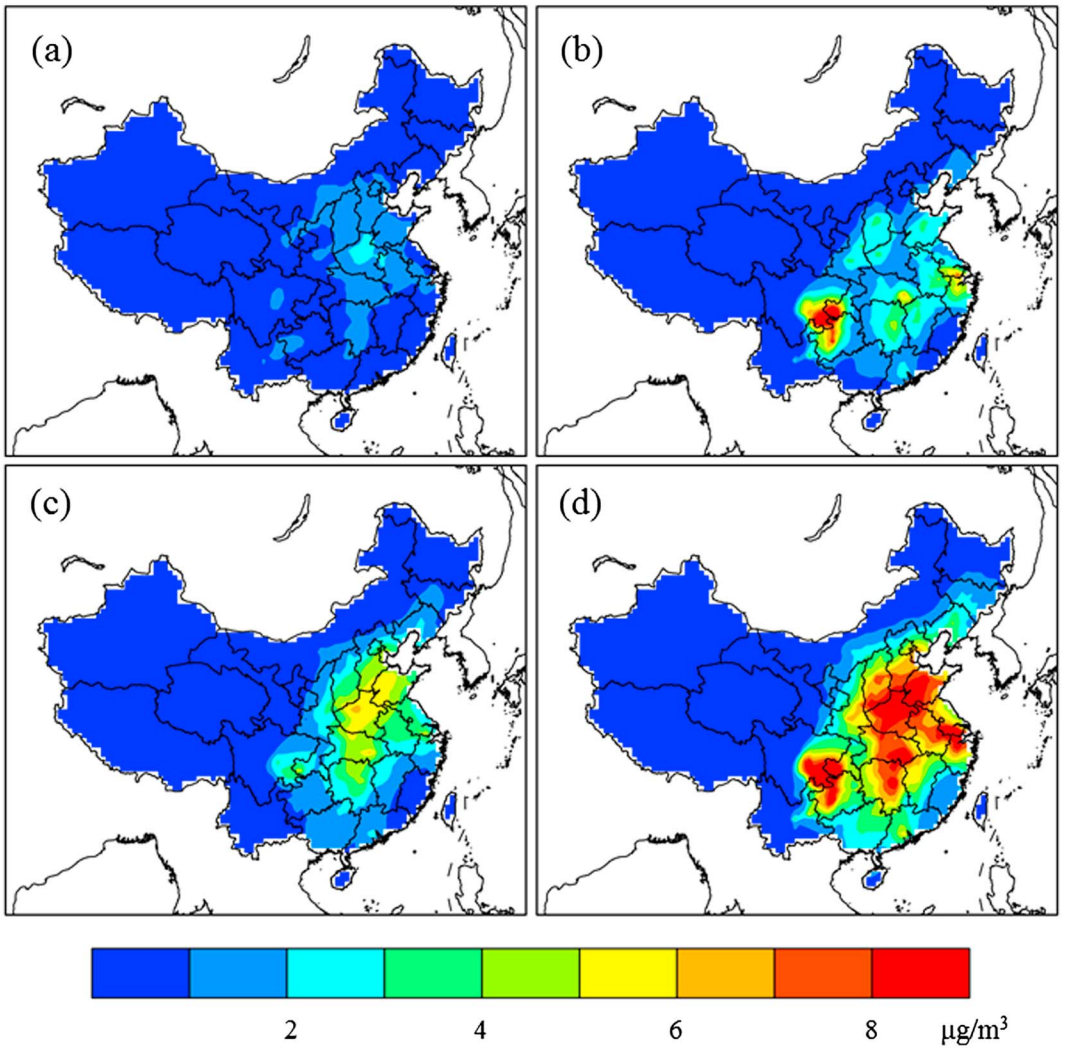

Figure 7. Spatial distribution of the increased sulfate concentrations ($\mu g\,m^{-3}$) caused by (a) Pathway I, (b) Pathway II, (c) Pathway III, and (d) sum of Pathways I, II, and III.

and Pathway II increased the daily average surface sulfate concentration by 4.2 $\mu g\,m^{-3}$ and 3.2 $\mu g\,m^{-3}$, respectively, while Pathway III contributed to an increase of 16.0 $\mu g\,m^{-3}$. Another haze event occurred on 25 December 2006 in Chengdu, Sichuan Basin. The daily average PM_{10} and sulfate concentrations were 325.9 $\mu g\,m^{-3}$ and 60.7 $\mu g\,m^{-3}$, respectively; the visibility was only 0.97 km. The measured relative humidity exceeded 90%. The simulated maximum daily average sulfate concentration was 64.1 $\mu g\,m^{-3}$ in Chengdu. The three additional sulfate production pathways related to mineral aerosol loadings contributed 3.4 $\mu g\,m^{-3}$, 17.6 $\mu g\,m^{-3}$, and 11.8 $\mu g\,m^{-3}$ to the sulfate concentration. This result indicates that the transition metal-catalyzed reaction can rapidly oxidize SO_2 and was the dominant sulfate enhancement pathway under high relative humidity conditions. A dust storm occurred on 9 March 2006, in the North China Plain. The observed mineral aerosol and sulfate concentrations were 415.9 $\mu g\,m^{-3}$ and 31.3 $\mu g\,m^{-3}$ in Gucheng. The simulated sulfate concentration was 26.0 $\mu g\,m^{-3}$. Although the mineral dust loading was high, the sulfate contribution from mineral aerosols was only 11.9 $\mu g\,m^{-3}$ because the relative humidity was as low as 37%.

4. Summary and Discussion

Our study integrated field measurements and numerical simulations to investigate the impact of mineral aerosols on sulfate production in China. WRF-Chem was improved by including the effects of mineral aerosols on sulfate production. The evaluations showed that the improved model performed well by

comparing the simulations with the measurements of sulfate concentrations at 14 sites, PM_{10} concentrations at two desert sites, observed pH values and Ca^{2+} concentrations in cloud water, ambient iron concentrations, and mineral cation concentrations. We conclude that mineral aerosols can facilitate transforming SO_2 to sulfate through three pathways. First, aqueous oxidation of S(IV) was enhanced by O_3, H_2O_2, and NO_2 with increasing amounts of SO_2 dissolved in cloud water because of water-soluble mineral cations. The increase in pH of cloud water promoted the dissolution of SO_2 and accelerated the oxidation with dissolved O_3 and NO_2 in the aqueous phase, especially in northern China with high NH_3 and NO_x emissions. The contribution by the first pathway to the national sulfate production was 5%. The second pathway was S(IV) catalyzed oxidation in the aqueous phase by transition metals rich in combustion mineral aerosols. The contribution to the annual sulfate production was 8%, with 19% during the winter that decreased to 2% during the summer. The third pathway is SO_2 heterogeneous reactions on the surface of mineral aerosols. The contribution to the national average sulfate concentration was 9% with 16% during the winter and a negligible effect during the summer. In total, mineral aerosol contributed a nationwide average of approximately 22% to sulfate production and was responsible for 40% of sulfate production during the winter and 12% during the summer in China.

Strong aqueous chemistry and heterogeneous uptake under humid and stagnant weather conditions could make the enhancement role much more efficient. Elevated sulfate concentrations result in thicker optical depths and stronger direct radiative forcing of sulfate. After diagnosing the direct radiative effect of individual aerosol species in the model [*C. Zhao et al*., 2013], our estimation indicated that the direct radiative effect of sulfate at the top of atmosphere (TOA) reached $-1.5\ W\ m^{-2}$ over China, greater than $-0.85\ W\ m^{-2}$ in the previous estimation [*Wang et al*., 2003]. Because of the tremendous consumption of coal and biofuel, a lot of attention has been given to the warming effect of BC in China [*Menon et al*., 2002; *Ramanathan and Carmichael*, 2008]. This enhanced sulfate cooling effect may play an important role in offsetting radiative warming caused by BC. Furthermore, several studies have shown that heterogeneous sulfate formation on mineral aerosol surfaces may change the loadings of externally mixed sulfate and reduce radiative-cooling effects [*Bauer and Koch*, 2005; *Bauer et al*., 2007]. Few climate models used in the Intergovernmental Panel on Climate Change Assessment Report fully accounted for the three pathways of sulfate production enhanced by mineral aerosols. Therefore, the radiative-cooling effect of sulfate may be underestimated, especially over polluted regions, such as China and India [*Ganguly et al*., 2009; *Park et al*., 2014; *Shekar Reddy et al*., 2004; *Verma et al*., 2012].

Previous simulations have often shown that sulfate is underestimated, while nitrate is overestimated in China [*Jiang et al*., 2013; *Kim et al*., 2006; *Park et al*., 2014; *Pozzer et al*., 2012]. In this study, the nitrate concentrations decreased with increasing sulfate production due to the three additional pathways. This finding indicates that the formation of ammonium sulfate and ammonium nitrate is still dominated by the NH_3-HNO_3-H_2SO_4 ternary system, in which ammonium sulfate is more stable than ammonium nitrate and forms first. This result is primarily attributed to sulfate being largely produced by photooxidation and aqueous oxidation (including transition metal-catalyzed oxidation). However, the heterogeneous reactions between acids and carbonates could impede the ammonium sulfate formation in the NH_3-HNO_3-H_2SO_4 ternary system when mineral aerosol loadings exceed a certain threshold [*Hsu et al*., 2014]. Acids can easily react with alkaline carbonates on mineral aerosols, and the excess acids adsorbed on the mineral aerosol surface are subsequently neutralized by ammonia. Ammonia can still play an important role even in the ammonium sulfate production through heterogeneous uptakes [*Song and Carmichael*, 1999; *Sullivan et al*., 2007].

Several uncertainties and limitations in the treatment of mineral aerosols exist in this study. The parameterization of catalyzed oxidation of S(IV) by transition metals was proposed by *Martin et al*. [1991], in which the catalyzed rates were derived for low S(IV), Fe(III), and Mn(II) concentrations at pH values of 3.0 and 5.0. More types of transition metals with high concentrations emitted from coal combustion may exist in the air in China, especially during winter. Additional experiments are needed to determine an appropriate rate expression for a wide range of pH values under high concentrations of transition metals. The uptake coefficient of SO_2 on the mineral aerosol surface may depend on temperature and relative humidity. Due to the large range of uptake coefficients for SO_2 in heterogeneous reactions that exist in the literature, several sensitivity simulations were conducted by varying the uptake coefficients to 1×10^{-5} and 1×10^{-4} under typical conditions and 5×10^{-5} and 5×10^{-4} for high humidity (RH $>$ 80%) to quantify the impact of uptake coefficients on sulfate production. The sensitivity simulations were conducted for January, when SO_2 and

mineral aerosol concentrations were both high. The results show that the sulfate concentrations produced from heterogeneous reactions were 0.4 $\mu g\,m^{-3}$ and 2.5 $\mu g\,m^{-3}$, respectively, when averaged over China. This result indicates that the uptake coefficients are critical for estimating sulfate production through heterogeneous reactions. More laboratory research is needed to better quantify the uptake coefficients of SO_2 on mineral aerosol surfaces. Furthermore, the surface saturation effect of heterogeneous sulfate production is not considered in this study and could be important in some cases. Some laboratory studies have shown that heterogeneous oxidation of SO_2 may be limited after initial reactions have occurred [*Baltrusaitis et al*., 2007; *Goodman et al*., 2001]. Further investigations are needed to study the surface saturation effect.

This study revealed that sulfate production maybe largely enhanced by catalyzed oxidation and heterogeneous uptake under high relative humidity conditions, significantly reducing the model's low sulfate concentration bias. However, more accurate estimates of SO_2 emissions, especially for residential coal combustion in northern China during wintertime, are needed for simulating sulfate concentrations.

Acknowledgments

Data to support this article can be acquired by contacting the corresponding author. This study is supported by National Natural Science Foundation of China (41275155 and 41121004), the Public Welfare Project for Environmental Protection (201309009), the projects 2010CB428501 and 2011CB403401 supported by Chinese Ministry of Science and Technology, the special fund of State Key Joint Laboratory of Environment Simulation and Pollution Control (14Y01ESPCP), and the Jiangsu Provincial 2011 Program (Collaborative Innovation Center of Climate Change). Chun Zhao acknowledges the support by the US DOE as part of the Regional and Global Climate Modeling program. The Pacific Northwest National Laboratory is operated for DOE by Battelle Memorial Institute under contract DE-AC05-76RL01830. The MODIS products are provided by Land Process Distributed Active Archive Center (LP-DAAC).

References

Alexander, B., R. J. Park, D. J. Jacob, and S. L. Gong (2009), Transition metal-catalyzed oxidation of atmospheric sulfur: Global implications for the sulfur budget, *J. Geophys. Res.*, *114*, D02309, doi:10.1029/2008JD010486.

Arimoto, R., X. Y. Zhang, B. J. Huebert, C. H. Kang, D. L. Savoie, J. M. Prospero, S. K. Sage, C. A. Schloesslin, H. M. Khaing, and S. N. Oh (2004), Chemical composition of atmospheric aerosols from Zhenbeitai, China, and Gosan, South Korea, during ACE-Asia, *J. Geophys. Res.*, *109*, D19S04, doi:10.1029/2003JD004323.

Baltrusaitis, J., D. M. Cwiertny, and V. H. Grassian (2007), Adsorption of sulfur dioxide on hematite and goethite particle surfaces, *Phys. Chem. Chem. Phys.*, *9*(41), 5542–5554, doi:10.1039/b709167b.

Bao, H., S. Yu, and D. Q. Tong (2010), Massive volcanic SO_2 oxidation and sulphate aerosol deposition in Cenozoic North America, *Nature*, *465*(7300), 909–912, doi:10.1038/nature09100.

Bates, T. S., et al. (2004), Marine boundary layer dust and pollutant transport associated with the passage of a frontal system over eastern Asia, *J. Geophys. Res.*, *109*, D19S19, doi:10.1029/2003JD004094.

Bauer, S. E., and D. Koch (2005), Impact of heterogeneous sulfate formation at mineral dust surfaces on aerosol loads and radiative forcing in the Goddard Institute for Space Studies general circulation model, *J. Geophys. Res.*, *110*, D17202, doi:10.1029/2005JD005870.

Bauer, S. E., M. I. Mishchenko, A. A. Lacis, S. Zhang, J. Perlwitz, and S. M. Metzger (2007), Do sulfate and nitrate coatings on mineral dust have important effects on radiative properties and climate modeling?, *J. Geophys. Res.*, *112*, D06307, doi:10.1029/2005JD006977.

Brandt, C., and R. van Eldik (1995), Transition-metal-catalyzed oxidation of sulfur(IV) oxides-atmospheric-relevant processes and mechanisms, *Chem. Rev.*, *95*(1), 119–190.

Cao, J., X. Tie, W. F. Dabberdt, T. Jie, Z. Zhao, Z. An, Z. Shen, and Y. Feng (2013), On the potential high acid deposition in northeastern China, *J. Geophys. Res. Atmos.*, *118*, 4834–4846, doi:10.1002/jgrd.50381.

Charlson, R. J., S. E. Schwartz, J. M. Hales, R. D. Cess, J. A. Coakley, J. E. Hansen, and D. J. Hofmann (1992), Climate forcing by anthropogenic aerosols, *Science*, *255*(5043), 423–430.

Chen, C., G. Liang, and X. Wang (2006), Chemical composition and sources of aerosol fine particles in Guangzhou, *Environ. Monitor. China*, *22*(5), 61–64.

Chen, H., A. Laskin, J. Baltrusaitis, C. A. Gorski, M. M. Scherer, and V. H. Grassian (2012), Coal fly ash as a source of iron in atmospheric dust, *Environ. Sci. Tech.*, *46*(4), 2112–2120.

Dai, S., L. Zhao, S. Peng, C.-L. Chou, X. Wang, Y. Zhang, D. Li, and Y. Sun (2010), Abundances and distribution of minerals and elements in high-alumina coal fly ash from the Jungar Power Plant, Inner Mongolia, China, *Int. J. Coal Geol.*, *81*(4), 320–332, doi:10.1016/j.coal.2009.03.005.

Dentener, F. J., G. R. Carmichael, Y. Zhang, J. Lelieveld, and P. J. Crutzen (1996), Role of mineral aerosol as a reactive surface in the global troposphere, *J. Geophys. Res.*, *101*(D17), 22,869–22,889, doi:10.1029/96JD01818.

Duvall, R., B. Majestic, M. Shafer, P. Chuang, B. Simoneit, and J. Schauer (2008), The water-soluble fraction of carbon, sulfur, and crustal elements in Asian aerosols and Asian soils, *Atmos. Environ.*, *42*(23), 5872–5884.

Fairlie, T. D., D. J. Jacob, J. E. Dibb, B. Alexander, M. A. Avery, A. V. Donkelaar, and L. Zhang (2010), Impact of mineral dust on nitrate, sulfate, and ozone in transpacific Asian pollution plumes, *Atmos. Chem. Phys.*, *10*(8), 3999–4012.

Fast, J. D., W. I. Gustafson Jr., R. C. Easter, R. A. Zaveri, J. C. Barnard, E. G. Chapman, and G. A. Grell (2006), Evolution of ozone, particulates, and aerosol direct forcing in an urban area using a new fully-coupled meteorology, chemistry, and aerosol model, *J. Geophys. Res.*, *111*, D21305, doi:10.1029/2005JD006721.

Fu, Q., G. Zhuang, J. Wang, C. Xu, K. Huang, J. Li, B. Hou, T. Lu, and D. G. Streets (2008), Mechanism of formation of the heaviest pollution episode ever recorded in the Yangtze River Delta, China, *Atmos. Environ.*, *42*(9), 2023–2036, doi:10.1016/j.atmosenv.2007.12.002.

Ganguly, D., P. Ginoux, V. Ramaswamy, D. M. Winker, B. N. Holben, and S. N. Tripathi (2009), Retrieving the composition and concentration of aerosols over the Indo-Gangetic basin using CALIOP and AERONET data, *Geophys. Res. Lett.*, *36*, L13806, doi:10.1029/2009GL038315.

Goodman, A. L., P. Li, C. R. Usher, and V. H. Grassian (2001), Heterogeneous uptake of sulfur dioxide on aluminum and magnesium oxide particles, *J. Phys. Chem. A*, *105*(25), 6109–6120.

Hao, Y., Z. Guo, Z. Yang, M. Fang, and J. Feng (2007), Seasonal variations and sources of various elements in the atmospheric aerosols in Qingdao, China, *Atmos. Res.*, *85*(1), 27–37.

Harris, E., B. Sinha, S. Foley, J. N. Crowley, S. Borrmann, and P. Hoppe (2012), Sulfur isotope fractionation during heterogeneous oxidation of SO_2 on mineral dust, *Atmos. Chem. Phys.*, *12*, 4867–4884.

Harris, E., B. Sinha, D. van Pinxteren, A. Tilgner, K. W. Fomba, J. Schneider, A. Roth, T. Gnauk, B. Fahlbusch, and S. Mertes (2013), Enhanced role of transition metal ion catalysis during in-cloud oxidation of SO_2, *Science*, *340*(6133), 727–730, doi:10.1126/science.1230911.

Haywood, J., and O. Boucher (2000), Estimates of the direct and indirect radiative forcing due to tropospheric aerosols: A review, *Rev. Geophys.*, *38*(4), 513–543, doi:10.1029/1999RG000078.

Hsu, S. C., C. S. L. Lee, C. A. Huh, R. Shaheen, F. J. Lin, S. C. Liu, M. C. Liang, and T. Jun (2014), Ammonium deficiency caused by heterogeneous reactions during a super Asian dust episode, *J. Geophys. Res. Atoms.*, *119*, 6803–6817, doi:10.1002/2013JD021096.

Huang, X., M. Li, J. Li, and Y. Song (2012a), A high-resolution emission inventory of crop burning in fields in China based on MODIS Thermal Anomalies/Fire products, *Atmos. Environ.*, *50*, 9–15.

Huang, X., Y. Song, M. Li, J. Li, Q. Huo, X. Cai, T. Zhu, M. Hu, and H. Zhang (2012b), A high-resolution ammonia emission inventory in China, *Global Biogeochem. Cycles*, *26*, GB1030, doi:10.1029/2011GB004161.

Hwang, H., and C. Ro (2006), Direct observation of nitrate and sulfate formations from mineral dust and sea-salts using low-Z particle electron probe X-ray microanalysis, *Atmos. Environ.*, *40*(21), 3869–3880, doi:10.1016/j.atmosenv.2006.02.022.

Jiang, H., H. Liao, H. O. T. Pye, S. Wu, L. J. Mickley, J. H. Seinfeld, and X. Y. Zhang (2013), Projected effect of 2000–2050 changes in climate and emissions on aerosol levels in China and associated transboundary transport, *Atmos. Chem. Phys.*, *13*, 7937–7960.

Jickells, T., Z. An, K. K. Andersen, A. Baker, G. Bergametti, N. Brooks, J. Cao, P. Boyd, R. Duce, and K. Hunter (2005), Global iron connections between desert dust, ocean biogeochemistry, and climate, *Science*, *308*(5718), 67–71.

Karl, T. R., and K. E. Trenberth (2003), Modern global climate change, *Science*, *302*(5651), 1719–1723, doi:10.1126/science.1090228.

Kiehl, J., and B. Briegleb (1993), The relative roles of sulfate aerosols and greenhouse gases in climate forcing, *Science*, *260*(5106), 311–314.

Kim, J. Y., C. H. Song, Y. S. Ghim, J. G. Won, S. C. Yoon, G. R. Carmichael, and J. H. Woo (2006), An investigation on NH_3 emissions and particulate NH_4^+-NO_3^- formation in East Asia, *Atmos. Environ.*, *40*(12), 2139–2150, doi:10.1016/j.atmosenv.2005.11.048.

Lei, Y., Q. Zhang, K. He, and D. G. Streets (2011), Primary anthropogenic aerosol emission trends for China, 1990–2005, *Atmos. Chem. Phys.*, *11*(3), 931–954.

Levin, Z., E. Ganor, and V. Gladstein (1996), The effects of desert particles coated with sulfate on rain formation in the eastern Mediterranean, *J. Appl. Meteorol.*, *35*(9), 1511–1523.

Li, L., Z. Chen, Y. Zhang, T. Zhu, J. Li, and J. Ding (2006), Kinetics and mechanism of heterogeneous oxidation of sulfur dioxide by ozone on surface of calcium carbonate, *Atmos. Chem. Phys.*, *6*(9), 2453–2464.

Li, M., Y. Song, X. Huang, J. Li, Y. Mao, T. Zhu, X. H. Cai, and B. Liu (2014), Improving mesoscale modeling using satellite-derived land surface parameters in the Pearl River Delta region, China, *J. Geophys. Res. Atoms.*, *119*, 6325–6346, doi:10.1002/2014JD021871.

Li, W. J., S. Z. Zhou, X. Wang, Z. Xu, C. Yuan, Y. C. Yu, Q. Z. Zhang, and W. X. Wang (2011), Integrated evaluation of aerosols from regional brown hazes over Northern China in Winter: Concentrations, sources, transformation, and mixing states, *J. Geophys. Res.*, *116*, D09301, doi:10.1029/2010JD015099.

Li, X. R., L. L. Wang, D. S. Ji, T. X. Wen, Y. P. Pan, Y. Sun, and Y. S. Wang (2013), Characterization of the size-segregated water-soluble inorganic ions in the Jing-Jin-Ji urban agglomeration: Spatial/temporal variability, size distribution and sources, *Atmos. Environ.*, *77*, 250–259, doi:10.1016/j.atmosenv.2013.03.042.

Liao, H., P. J. Adams, S. H. Chung, J. H. Seinfeld, L. J. Mickley, and D. J. Jacob (2003), Interactions between tropospheric chemistry and aerosols in a unified general circulation model, *J. Geophys. Res.*, *108*(D1), 4001, doi:10.1029/2001JD001260.

Liu, C., J. Zhang, and Z. Shen (2002), Spatial and temporal variability of trace metals in aerosol from the desert region of China and the Yellow Sea, *J. Geophys. Res.*, *107*(D14), 4215, doi:10.1029/2001JD000635.

Lu, Z., Q. Zhang, and D. G. Streets (2011), Sulfur dioxide and primary carbonaceous aerosol emissions in China and India, 1996–2010, *Atmos. Chem. Phys.*, *11*(18), 9839–9864, doi:10.5194/acp-11-9839-2011.

Manktelow, P. T., K. S. Carslaw, G. W. Mann, and D. V. Spracklen (2010), The impact of dust on sulfate aerosol, CN and CCN during an East Asian dust storm, *Atmos. Chem. Phys.*, *10*, 365–382.

Martin, L. R., and T. W. Good (1991), Catalyzed oxidation of sulfur dioxide in solution: The iron-manganese synergism, *Atmos. Environ.*, *25A*(10), 2395–2399.

Martin, L. R., M. W. Hill, A. F. Tai, and T. W. Good (1991), The iron catalyzed oxidation of sulfur (IV) in aqueous solution: Differing effects of organics at high and low pH, *J. Geophys. Res.*, *96*(D2), 3085–3097, doi:10.1029/90JD02611.

Matsuki, A., et al. (2005), Morphological and chemical modification of mineral dust: Observational insight into the heterogeneous uptake of acidic gases, *Geophys. Res. Lett.*, *32*, L22806, doi:10.1029/2005GL024176.

Menon, S., J. Hansen, L. Nazarenko, and Y. Luo (2002), Climate effects of black carbon aerosols in China and India, *Science*, *297*(5590), 2250–2253, doi:10.1126/science.1075159.

Mori, I., Y. Iwasaka, K. Matsunaga, M. Hayashi, and M. Nishikawa (1999), Chemical characteristics of free tropospheric aerosols over the Japan Sea coast: Aircraft-borne measurements, *Atmos. Environ.*, *33*(4), 601–609, doi:10.1016/S1352-2310(98)00262-3.

National Bureau of Statistics of China (2013), *China Statistical Yearbook*, China Statistics Press, Beijing.

Pandis, S. N., and J. H. Seinfeld (1989), Mathematical modeling of acid deposition due to radiation fog, *J. Geophys. Res.*, *94*(D10), 12,911–12,923, doi:10.1029/JD094iD10p12911.

Park, R., S. Lee, S. Shin, and C. Song (2014), Contribution of ammonium nitrate to aerosol optical depth and direct radiative forcing by aerosols over East Asia, *Atmos. Chem. Phys.*, *14*, 2185–2201, doi:10.5194/acp-14-2185-2014.

Paulot, F., D. J. Jacob, R. W. Pinder, J. O. Bash, K. Travis, and D. K. Henze (2014), Ammonia emissions in the United States, European Union, and China derived by high-resolution inversion of ammonium wet deposition data: Interpretation with a new agricultural emissions inventory (MASAGE_NH3), *J. Geophys. Res. Atmos.*, *119*, 4343–4364, doi:10.1002/2013JD021130.

Pozzer, A., A. de Meij, K. J. Pringle, H. Tost, U. M. Doering, J. van Aardenne, and J. Lelieveld (2012), Distributions and regional budgets of aerosols and their precursors simulated with the EMAC chemistry-climate model, *Atmos. Chem. Phys.*, *12*, 961–987.

Qian, Y., and F. Giorgi (1999), Interactive coupling of regional climate and sulfate aerosol models over eastern Asia, *J. Geophys. Res.*, *104*(D6), 6477–6499, doi:10.1029/98JD02347.

Qian, Y., D. Gong, J. Fan, L. R. Leung, R. Bennartz, D. Chen, and W. Wang (2009), Heavy pollution suppresses light rain in China: Observations and modeling, *J. Geophys. Res.*, *114*, D00K02, doi:10.1029/2008JD011575.

Ramanathan, V., and G. Carmichael (2008), Global and regional climate changes due to black carbon, *Nat. Geosci.*, *1*(4), 221–227, doi:10.1038/ngeo156.

Seinfeld, J. H., and S. N. Pandis (2006), *Atmospheric Chemistry and Physics: From Air Pollution to Climate Change*, Wiley, New York.

Shaw, W. J., K. J. Allwine, B. G. Fritz, F. C. Rutz, J. P. Rishel, and E. G. Chapman (2008), Evaluation of the wind erosion module in DUSTRAN, *Atmos. Environ.*, *42*(8), 1907–1921, doi:10.1016/j.atmosenv.2007.11.022.

Shekar Reddy, M., O. Boucher, C. Venkataraman, S. Verma, J.-F. Leon, N. Bellouin, and M. Pham (2004), General circulation model estimates of aerosol transport and radiative forcing during the Indian Ocean Experiment, *J. Geophys. Res.*, *109*, D16205, doi:10.1029/2004JD004557.

Shen, Z., Y. Wu, H. Xiao, C. Bai, and M. Huang (1993), Some basic features of cloudwater chemistry in the southwest area of China [in Chinese], *Chin. J. Atmos. Sci.*, *17*(1), 87–96.

Siefert, R. L., A. M. Johansen, M. R. Hoffmann, and S. O. Pehkonen (1998), Measurements of trace metal (Fe, Cu, Mn, Cr) oxidation states in fog and stratus clouds, *J. Air Waste Manag. Assoc.*, *48*(2), 128–143.

Song, C. H., and G. R. Carmichael (1999), The aging process of naturally emitted aerosol (sea-salt and mineral aerosol) during long range transport, *Atmos. Environ.*, *33*(14), 2203–2218.
Song, C. H., K. Maxwell-Meier, R. J. Weber, V. Kapustin, and A. Clarke (2005), Dust composition and mixing state inferred from air-borne composition measurements during ACE-Asia C130 Flight #6, *Atmos. Environ.*, *39*(2), 359–369.
Song, Y., D. Chang, B. Liu, W. J. Miao, L. Zhu, and Y. H. Zhang (2010), A new emission inventory for nonagricultural open fires in Asia from 2000 to 2009, *Environ. Res. Lett.*, *5*(1), 014014, doi:10.1088/1748-9326/5/1/014014.
Stocker, T. F., G.-K. P. D. Qin, M. Tignor, S. K. Allen, J. Boschung, A. Nauels, Y. Xia, and V. B. A. P. M. Midgley (Eds.) (2013), *Climate Change 2013: The Physical Science Basis. Contribution of Working Group I to the Fifth Assessment Report of the Intergovernmental Panel on Climate Change*, 127 pp., Cambridge Univ. Press, Cambridge, New York.
Sullivan, R. C., S. A. Guazzotti, D. A. Sodeman, and K. A. Prather (2007), Direct observations of the atmospheric processing of Asian mineral dust, *Atmos. Chem. Phys.*, *7*, 1213–1226.
Sun, Y., G. Zhuang, A. Tang, Y. Wang, and Z. An (2006), Chemical characteristics of $PM_{2.5}$ and PM_{10} in haze-fog episodes in Beijing, *Environ. Sci. Tech.*, *40*(10), 3148–3155, doi:10.1021/es051533g.
Ullerstam, M., M. S. Johnson, R. Vogt, and E. Ljungstrom (2003), DRIFTS and Knudsen cell study of the heterogeneous reactivity of SO_2 and NO_2 on mineral dust, *Atmos. Chem. Phys.*, *3*, 2043–2051.
Usher, C. R., A. E. Michel, and V. H. Grassian (2003), Reactions on mineral dust, *Chem. Rev.*, *103*(12), 4883–4939, doi:10.1021/Cr020657y.
Van Damme, M., L. Clarisse, C. L. Heald, D. Hurtmans, Y. Ngadi, C. Clerbaux, A. J. Dolman, J. W. Erisman, and P. F. Coheur (2014), Global distributions, time series and error characterization of atmospheric ammonia (NH_3) from IASI satellite observations, *Atmos. Chem. Phys.*, *14*, 2905–2922, doi:10.5194/acp-14-2905-2014.
Verma, S., O. Boucher, M. Shekar Reddy, H. C. Upadhyaya, P. Le Van, F. S. Binkowski, and O. P. Sharma (2012), Tropospheric distribution of sulphate aerosols mass and number concentration during INDOEX-IFP and its transport over the Indian Ocean: A GCM study, *Atmos. Chem. Phys.*, *12*, 6185–6196.
Wang, T. J., J. Z. Min, Y. F. Xu, and K. S. Lam (2003), Seasonal variations of anthropogenic sulfate aerosol and direct radiative forcing over China, *Meteorol. Atmos. Phys.*, *84*(3), 185–198, doi:10.1007/s00703-002-0581-7.
Wang, X., W. Wang, L. Yang, X. Gao, W. Nie, Y. Yu, P. Xu, Y. Zhou, and Z. Wang (2012), The secondary formation of inorganic aerosols in the droplet mode through heterogeneous aqueous reactions under haze conditions, *Atmos. Environ.*, *63*, 68–76, doi:10.1016/j.atmosenv.2012.09.029.
Winchester, J. W., L. Weixiu, R. Lixin, W. Mingxing, and W. Maenhaut (1981), Fine and coarse aerosol composition from a rural area in north China, *Atmos. Environ.*, *15*(6), 933–937.
Xuan, J., and I. N. Sokolik (2002), Characterization of sources and emission rates of mineral dust in Northern China, *Atmos. Environ.*, *36*(31), 4863–4876, doi:10.1016/S1352-2310(02)00585-X.
Xue, L., A. Ding, Y. Ren, J. Gao, T. Wang, W. Wang, X. Wang, H. Lei, and D. Jin (2010), Aircraft study of cloud water chemistry over Jilin Province in Northeast China [in Chinese], *China Environ. Sci.*, *9*, 1162–1167.
Yang, L., X. Zhou, Z. Wang, Y. Zhou, S. Cheng, P. Xu, X. Gao, W. Nie, X. Wang, and W. Wang (2012), Airborne fine particulate pollution in Jinan, China: Concentrations, chemical compositions and influence on visibility impairment, *Atmos. Environ.*, *55*, 506–514.
Yao, X., C. K. Chan, M. Fang, S. Cadle, T. Chan, P. Mulawa, K. He, and B. Ye (2002), The water-soluble ionic composition of $PM_{2.5}$ in Shanghai and Beijing, China, *Atmos. Environ.*, *36*(26), 4223–4234.
Ye, B., X. Ji, H. Yang, X. Yao, C. K. Chan, S. H. Cadle, T. Chan, and P. A. Mulawa (2003), Concentration and chemical composition of $PM_{2.5}$ in Shanghai for a 1-year period, *Atmos. Environ.*, *37*(4), 499–510.
You, C., and X. Xu (2010), Coal combustion and its pollution control in China, *Energy*, *35*(11), 4467–4472, doi:10.1016/j.energy.2009.04.019.
Zhang, D. Z., and Y. Iwasaka (1999), Nitrate and sulfate in individual Asian dust-storm particles in Beijing, China in spring of 1995 and 1996, *Atmos. Environ.*, *33*(19), 3213–3223.
Zhang, Q., D. G. Streets, K. He, Y. X. Wang, A. Richter, J. P. Bur- rows, I. Uno, C. J. Jang, D. Chen, Z. Yao, and Y. Lei (2007), NO_x emission trends for China, 1995–2004: The view from the ground and the view from space, *J. Geophys. Res.*, *112*, D22306, doi:10.1029/2007JD008684.
Zhang, Q., D. G. Streets, G. R. Carmichael, K. He, H. Huo, A. Kannari, Z. Klimont, I. Park, S. Reddy, and J. Fu (2009), Asian emissions in 2006 for the NASA INTEX-B mission, *Atmos. Chem. Phys.*, *9*(14), 5131–5153, doi:10.5194/acp-9-5131-2009.
Zhang, Q., K. He, and H. Huo (2012a), Policy: Cleaning China's air, *Nature*, *484*(7393), 161–162, doi:10.1038/484161a.
Zhang, W., D. Shao, A. Shen, Z. He, M. Huang, Z. Shen, and Y. Wu (1991), Analysis of chemical compositions of cloud water and rain water during the plum rains period in Shanghai [in Chinese], *J. Appl. Meterol. Sci.*, *2*(4), 375–384.
Zhang, X., G. Zhuang, J. Chen, Y. Wang, X. Wang, Z. An, and P. Zhang (2006), Heterogeneous reactions of sulfur dioxide on typical mineral particles, *J. Phys. Chem. B*, *110*(25), 12,588–12,596.
Zhang, X., Y. Wang, T. Niu, X. Zhang, S. Gong, Y. Zhang, and J. Sun (2012b), Atmospheric aerosol compositions in China: Spatial/temporal variability, chemical signature, regional haze distribution and comparisons with global aerosols, *Atmos. Chem. Phys.*, *12*(2), 779–799, doi:10.5194/acp-12-779-2012.
Zhang, X. Y., R. Arimoto, and Z. S. An (1997), Dust emission from Chinese desert sources linked to variations in atmospheric circulation, *J. Geophys. Res.*, *102*(D23), 28,041–28,047, doi:10.1029/97JD02300.
Zhao, C., X. Liu, L. R. Leung, B. Johnson, S. A. McFarlane, W. I. Gustafson Jr., J. D. Fast, and R. Easter (2010), The spatial distribution of mineral dust and its shortwave radiative forcing over North Africa: Modeling sensitivities to dust emissions and aerosol size treatments, *Atmos. Chem. Phys.*, *10*, 8821–8838.
Zhao, C., L. Ruby Leung, R. Easter, J. Hand, and J. Avise (2013), Characterization of speciated aerosol direct radiative forcing over California, *J. Geophys. Res. Atmos.*, *118*, 2372–2388, doi:10.1029/2012JD018364.
Zhao, P., Y. Feng, T. Zhu, and J. Wu (2006), Characterizations of resuspended dust in six cities of North China, *Atmos. Environ.*, *40*(30), 5807–5814, doi:10.1016/j.atmosenv.2006.05.026.
Zhao, P. S., F. Dong, D. He, X. J. Zhao, X. L. Zhang, W. Z. Zhang, Q. Yao, and H. Y. Liu (2013), Characteristics of concentrations and chemical compositions for $PM_{2.5}$ in the region of Beijing, Tianjin, and Hebei, China, *Atmos. Chem. Phys.*, *13*(9), 4631–4644, doi:10.5194/acp-13-4631-2013.
Zhao, X. J., P. S. Zhao, J. Xu, W. Meng, W. W. Pu, F. Dong, D. He, and Q. F. Shi (2013), Analysis of a winter regional haze event and its formation mechanism in the North China Plain, *Atmos. Chem. Phys.*, *13*, 5685–5696, doi:10.5194/acp-13-5685-2013.